A novel quantification method for RPE phagocytosis using a VLC-PUFA-based strategy

Fangyuan Gao[1]*, Emily Tom[2]*, Dorota Skowronska-Krawczyk[1,2] ✉

[1] Department of Ophthalmology, Center for Translational Vision Research, School of Medicine, UC Irvine, Irvine, CA

[2] Department of Physiology and Biophysics, Department of Ophthalmology, Center for Translational Vision Research, School of Medicine, UC Irvine, Irvine, CA

* equal contribution

KEYWORDS Retinal pigment epithelium (RPE), phagocytosis, very-long-chain polyunsaturated fatty acids (VLC-PUFA), Liquid Chromatography-Mass Spectrometer (LC-MS), quantification

✉ corresponding author: dorotask@hs.uci.edu

ABSTRACT

The retinal pigment epithelium (RPE) lies adjacent to the photoreceptors and is responsible for the engulfment and degradation of shed photoreceptor outer segment fragments (POS) through receptor-mediated phagocytosis. Phagocytosis of POS is critical for maintaining photoreceptor function and is a key indicator of RPE functionality. The current methods to study RPE phagocytosis are not compatible with direct quantification with high sensitivity that can be applied in a high-throughput manner. To overcome some of these limitations, we have developed a novel VLC-PUFA-based approach for evaluating RPE phagocytic activity in primary bovine RPE and ARPE-19 cells and validated its results by traditional methods. This new approach can be used to detect the dynamic process of phagocytosis at varying POS concentrations and incubation times and offers a robust, quantifiable, and unbiased assay for high-throughput screening.

INTRODUCTION

Phagocytosis of photoreceptor outer segment (POS) by the retinal pigment epithelium (RPE) is essential for retinal health and function. Disruptions in phagocytosis have been previously linked to retinal degeneration in inherited retinal diseases, aging, and age-related macular degeneration (AMD)(Gal, Li et al. 2000, Sun, Cai et al. 2007, Inana, Murat et al. 2018). Due to the importance of this process in maintaining visual function, it has remained an area of intense study, and several techniques, both *in situ* and *in vitro*, have been developed over the past 50 years to quantify RPE phagocytosis. Common *in situ* methods to study RPE phagocytosis have been recently reviewed (Vargas and Finnemann 2022). Briefly, light microscopy(LaVail 1976), transmission electron microscopy (TEM)(Young 1978), and immuno-electron microscopy (Lewis, Kundinger et al. 2018) allow for visualization of phagosomes within RPE. While *in situ* methods provide valuable insight into candidate proteins that may be important in POS renewal in animal models such as mice with different mutations, evaluating POS uptake by cultured RPE cells *in vitro* possesses several potential applications and advantages: (1) Defects in RPE or photoreceptor function during the normally synchronized process of phagocytosis can be separated from one another. (2) Depending on the gene or protein of interest, different phases of the phagocytic process, namely particle recognition/binding, internalization, and digestion, can be distinguished (Mao and Finnemann 2012). (3) Using genetic or pharmacological approaches, RPE cells can be manipulated to simulate an *in vivo* RPE cell-specific disease state(Tagawa, Ikeda et al. 2021). (4) High-throughput screen platforms can be established to rescue phagocytosis deficiency in RPE (Schreiter, Vafia et al. 2020). The current methods to quantify POS uptake by RPE cells in culture include fluorescence-based assays, such as fluorescence-activated cell sorting (FACS)(Ramarao and Meyer 2001), fluorescence scanning(Hook and Odeyale 1989), or immunofluorescence(Mao and Finnemann 2012), which require POS to be first labeled with a fluorescent dye such as FITC, and immunoblot-based assays, where unlabeled POS can be detected using an antibody specific to POS, such as transducin (Sethna, Chamakkala et al. 2016) or rhodopsin (Tagawa, Ikeda et al. 2021).

Fluorescence- and immunoblot-based assays allow for the discrimination of surface-bound and engulfed POS particles (Mao and Finnemann 2012). However, these assays possess several general limitations. First, fluorescence-based phagocytosis assays are dependent on POS preparation and fluorescence conjugation, limiting interexperimental comparisons. Furthermore, the quantification of POS uptake based on images is often carried out by visual inspection and is therefore time-consuming, subjective, and expensive. Based on the choice of POS protein antibody, detection of POS-specific markers in protein lysates by immunoblot exhibits experimental variability. For example, different monoclonal antibodies to rhodopsin recognize either the C- or N-terminus of rhodopsin, and these epitopes are degraded at different rates due to their varying stability during phagocytosis (Esteve-Rudd, Lopes et al. 2014). These inherent limitations highlight the critical need for a more efficient analysis method with less experimental bias and interexperimental variability to complement the existing assays.

In the retina, very-long-chain polyunsaturated fatty acids (VLC-PUFAs, which contain acyl chains longer than 26 carbons) are produced in photoreceptors through the elongation of LC-PUFAs mediated by

Elongation of very-long-chain fatty acids like-4 (ELOVL4) and are highly enriched in the light-sensitive membrane disks of the photoreceptor outer segments(Agbaga, Brush et al. 2008, Sander, Sears et al. 2021). Following shedding and subsequent phagocytosis of photoreceptor outer segments by RPE cells, photoreceptor-derived VLC-PUFAs are efficiently recycled back to the inner segments of photoreceptors for further use (Lewandowski, Sander et al. 2021).

Here, we present direct evidence that RPE cells do not produce or maintain VLC-PUFAs endogenously. Based on this finding, we developed a novel phagocytosis assay based on the quantification of phagocytosed VLC-PUFAs by RPE cells. The proposed VLC-PUFA-based assay has the ability to quantify the efficiency of phagocytosis in RPE cells in culture after incubation with different concentrations of ROS and different incubation times. This new method is also suitable for the quantification of defects in RPE phagocytic activity caused by simultaneous knockdown of three ligands in phagocytosis. The results obtained using this VLC-PUFA-based assay were complementary to traditional immunofluorescence- and immunoblot-based methods, providing a rapid, quantitative, and high-throughput method for the evaluation of phagocytosis in RPE cells.

MATERIALS AND METHODS

Cell culture and siRNA transfection

ARPE-19 cells were obtained from ATCC and maintained in DMEM/F-12 containing 10% fetal bovine serum (FBS). Primary bovine retinal pigment epithelial cells (RPE) were generated by Dr. Huajun Yan and maintained in RtEBM (Lonza, USA) supplemented with RtEGM SingleQuots Supplement Pack (Lonza, USA). Both cell lines were incubated at 37 °C with 5% CO_2. ARPE-19 cells and primary bovine RPE cells were seeded in 12-well plates and grown to full confluency before experiments.

ARPE-19 cells were electroporated with three unique siRNA specific for human *MERTK*, *GAS6*, and *MFGE8* (Table 1, Integrated DNA Technologies(IDT), USA), and cells electroporated without siRNA was used as a negative control, using Neon™ Transfection System (Thermo Fisher, USA) according to the manufacturer's protocol. Experiments were carried out 5 days after the transfection procedure. The effectiveness of the *MERTK*, *GAS6*, and *MFGE8* knockdown was examined using quantitative RT-PCR (qRT-PCR).

RNA Extraction, Reverse Transcription, and qPCR Analysis

Total RNA was extracted from cells using RNeasy Plus mini kits (Qiagen). RNA concentration was measured by a Qubit fluorescence assay (Thermo Fisher, USA). A total 1 µg of extracted RNA was reverse transcribed using SuperScript IV VILO Master Mix kit (Thermo Fisher, USA), according to manufacturer's instructions. cDNA was diluted 1:10 in nuclease free water prior to qPCR analysis using a CFX384 real-time PCR system (Bio-Rad, USA). Reaction mixtures containing 5 µl PowerUp STBR Green Master Mix (Applied Biosystems, USA), 4 µl cDNA, 1 µl primer mix (final concentration of 200 nM per primer) were prepared in Hard-Shell PCR 384-well plates (Bio-Rad, USA). Amplification conditions were as follows: 50 °C for 2 min, followed by 40 cycles at 95 °C for 15 s and 60 °C for 60 s. Melting curve analysis was performed from 65–95 °C. All samples were run in triplicate and mean Ct (cycle

threshold) values were used for further analysis.

Lipid purification and fatty acid extraction from RPE cells and tissue

Cell pellets were resuspended in 200 μL ddH_2O and transferred into a clean glass test tube. 1 μg 6Z,9Z,12Z,15Z,18Z-heneicosapentaenoic acid (FA 21:5, Cayman, USA) was added as internal standard. Lipids were extracted by the Bligh-Dyer method followed by hydrolysis and extraction of total fatty acids. Briefly, 750 μL ice-cold 1:2 (v/v) $CHCl_3$:MeOH was added directly to the sample and the sample was vortexed. Then 250 μL $CHCl_3$ was added and mixed well. 250 μL ddH_2O was added and vortexed well to produce a two-phase system. After centrifuging at 3000 RPM for 3 min, the bottom phase was collected and evaporated under a constant stream of nitrogen. To recover the total fatty acids, 720 μL acetonitrile and 10 μL hydrochloric acid were added to the dried film and the sample was kept at 95 °C for 1 h. Then, 1 ml of hexane was added to the sample and vortexed. The upper phase containing total fatty acids was transferred to a new tube and evaporated under nitrogen. The total fatty acids were dissolved in acetonitrile-isopropanol (50:50, v/v) for further LC-MS Analysis (**Fig. 1A**).

Tissue samples were homogenized in ddH_2O. 1 μg FA 21:5 was added as internal standard. Lipids were extracted by the Bligh-Dyer method followed by hydrolysis and extraction of total fatty acids was performed as described above.

ROS Phagocytosis Assay

RPE cells were seeded at equal density on 12-well plates to have at least triplicate samples for each condition. Then, the RPE cells were cultured in the cell culture incubator until they were fully confluent.

Bovine ROS (InVision BioResources) was counted and resuspended in cell culture medium. ROS aliquots were stored at -80 °C. For phagocytosis assays, cell number was determined, and appropriate ROS concentration (ROS/cell) was added. RPE cells were incubated with ROS in the cell culture incubator for the appropriate time. Phagocytosis was terminated by washing 3 times with PBS. To detect internalized ROS only by VLC-PUFA-based assay, trypsin containing EDTA (0.25%) was added to RPE cells and incubated in the cell culture incubator until the cells were transparent, but still attached. Trypsin-EDTA, along with most of the surface-bound ROS, was removed and the cells were then harvested and washed with PBS for 3 times. The cell pellet was kept at -20°C for further analysis.

LC-MS Analysis of VLC-PUFAs

Separation of VLC-PUFAs was achieved on an Acquity UPLC® BEH C18 column (1.7 μm, 2.1 mm × 100 mm, Waters Corporation) using a mobile phase consisting of 1% 1 mol/L ammonium acetate and 0.1% formic acid in water (A) acetonitrile/isopropanol (1:1, v/v), 1% 1 mol/L ammonium acetate, and 0.1% formic acid (B) at a flow rate of 0.4 mL/min, with the following linear gradient: 0-2 min, 35% -80% B, 2-7 min, 80-100% B,7-14 min, 100% B, 14-15,100-35% B.

For VLC-PUFAs analyses, 14Z,17Z,20Z,23Z,26Z,29Z-dotriacontahexaenoic acid (32:6, Cayman, USA) and the extracted mixed VLC-PUFAs from bovine retina was used as VLC-PUFA standards. The identification of each VLC-PUFA in retina samples was conducted extracting a chromatographic peak for each of the corresponding $[M-H]^-$ ions using 5 ppm tolerant in full scan mode. Then fragments of the different VLC-PUFAs were studied through a separated parallel reaction monitoring (PRM) method for

further identification of the compounds.

The established retention times were used for identification of LC-PUFAs and VLC-PUFAs in phagocytosed ROS (Table 2). For quantification, the Q Exactive MS (Thermo Fisher Scientific, Waltham, MA) was operated in a full MS scan mode (resolution 70,000) in negative mode with a scan range of m/z 250–800, then the interested VLC-PUFAs were quantified by extracting a chromatographic peak for the corresponding $[M-H]^-$ ions using 5 ppm tolerant. The comparison was made by normalizing each peak area with the internal standard fatty acid 21:5.

Quantification of phagocytosed ROS by immunocytochemical analysis

Immunofluorescence quantification of ROS phagocytosis was performed following a previously established protocol (Mao and Finnemann 2012). Briefly, confluent ARPE-19 monolayers grown on coverslips were incubated with 5, 10, or 20 FITC-conjugated ROS/cell for 2 and 5 hours. Washed cells were briefly fixed in 4% PFA in PBS for 20 min and the remaining fixative was quenched with NH_4Cl. Cells were blocked in 1% BSA for 10 min and incubated with mouse-1D4 antibody diluted in 1% BSA for 25 min. After washing 3 times in PBS, cells were incubated with goat anti-mouse AlexaFluor-647 secondary antibody diluted in 1% BSA for 1 hour. After washing 3 times in PBS, nuclei were stained with DAPI, and coverslips were mounted with Fluoromount G. Images were acquired using Keyence All-in-One Fluorescence Microscope (BZ-X800, Osaka, Japan) at 100X magnification, and the number of green particles was counted and normalized to the number of cell nuclei using single extract colocalization in Keyence Hybrid Cell Count software.

Quantification of phagocytosed ROS by Western Blot

Opsin immunoblotting was performed following a previously established protocol (Mao and Finnemann 2012). First, ROS were fluorescently labelled using standard kit (FITC 'Isomer I'/Invitrogen). Confluent ARPE-19 monolayers were incubated with 10 ROS/cell for 2 hours. Triplicate samples were designated for detection of either total (bound plus internal) ROS or only internalized ROS. Samples designated for total ROS detection were washed with PBS-CM (PBS with calcium and magnesium), while only internalized ROS samples were incubated with PBS-EDTA for 10 minutes. Total protein was extracted with ice-cold lysis buffer (20mM HEPES pH 7.9, 420mM NaCl, 3mM $MgCl_2$, 10% glycerol with freshly supplemented 5mM DTT and protease inhibitor cocktail), subjected to SDS-PAGE electrophoresis, transferred onto a PVDF membrane, and blocked with casein in PBS for 1 hour. The membrane was incubated with mouse-1D4 antibody overnight at 4 °C. Following 3 washes with PBST, the membrane was incubated with HRP-conjugated secondary antibodies for 1 hour. The bands were visualized by a chemiluminescent reaction and imaged using the ChemiDoc Imaging System. Densitometric analysis of obtained bands was performed by FIJI, and the data were normalized to total protein stained by Ponceau S.

RESULTS

VLC-PUFA quantification - method development

The quantification of VLC-PUFAs remains challenging due to their low abundance and the lack of commercial standards. The procedures most widely used for determining VLC-PUFA levels are Gas Chromatography-Mass Spectrometer (GC-MS) and GC-flame ionization detection following methyl-esterification (Agbaga, Brush et al. 2008, Tagawa, Ikeda et al. 2021). These methods are highly reproducible and are able to distinguish between n-3 and n-6 VLC-PUFAs; however, because they require esterification, they are not suitable for the detection of VLC-FAs that have poor volatility(Takashima, Toyoshi et al. 2020). To overcome these barriers, a Liquid Chromatography-Mass Spectrometer (LC-MS) method was developed to establish retention times of LC-PUFAs and VLC-PUFAs by using a standard VLC-PUFA, 14Z,17Z,20Z,23Z,26Z,29Z-dotriacontahexaenoic acid (32:6), and the extracted mixed VLC-PUFAs from bovine retina as VLC-PUFA standards (**Table 2**).

To obtain the PUFA composition from different samples, LC-PUFAs and VLC-PUFAs in samples were extracted and detected by using the established retention times in full scan (m/z 250–800) MS under negative mode (**Fig. 1A**). The identification of each VLC-PUFA (e.g. from bovine retina samples) was achieved through extraction of a chromatographic peak for each of the corresponding $[M-H]^-$ ions (**Fig.1B**) in full scan (FS) mode. Then, a separate parallel reaction monitoring (PRM) method was also used to obtain the fragments of different VLC-PUFA peaks for identification. After increasing collision energy, VLC-PUFAs derived peak clusters with a mass difference of 14 Da corresponding to CH_2, indicating a chain cleavage of double bonds (**Fig S1A, B**). The linear range and reproducibility of the FS mode-based quantification were further evaluated by using 32:6 and fatty acid extract, respectively. For 32:6, the linear range was from 50 nmol/L to 1000 nmol/L with a correlation coefficient of 0.994, and the limit of quantification was 5 nmol/L (**Fig. S1C**). The standard deviations of the peak area of the interested VLC-PUFAs of bovine retina extract were below 15% (n=5) (**Fig. S1D**) Bovine and mouse eyecups, as well as RPE cells isolated directly from eyecups, exhibited a high abundance of VLC-PUFAs ranging from 32:4 to 36:6, and the composition resembles that of retina tissue and ROS (**Fig. 1C** and **Fig. S1E**). On the contrary, cultured RPE cells, such as the widely used ARPE-19 cell line, primary bovine RPE cells, and human induced pluripotent stem cell iPSCs-derived RPE have minimal amounts of endogenous VLC-PUFAs (**Fig. 1D**), despite expressing genes involved in elongation of LC-PUFA – *ELOVL2* and *ELOVL4* (**Fig. 1D, inset**). This suggests that VLC-PUFAs in isolated RPE cells most probably originated from phagocytosed POS *in vivo*. Therefore, the deficiency of VLC-PUFAs in cultured RPE cells suggested the feasibility of using abundance of VLC-PUFAs as a measure of phagocytosis activity in RPE cells.

Quantification of phagocytosis in RPE cells

To evaluate the feasibility of the VLC-PUFA-based method for phagocytosis quantification, we followed the workflow presented in **Fig. 2A**. Briefly, ARPE-19 and primary bovine RPE cells were plated at equal density and grown to confluency in 12 well plates. Then, the ARPE-19 and primary bovine RPE cells were exposed to 20 ROS/cell for 5 h and 0.5h, respectively, following previously published protocols (Mao and Finnemann 2012). To terminate phagocytosis, cells were washed 3 times with PBS,

trypsinized to remove free and bound ROS (Westenskow, Moreno et al. 2012) and collected for analysis. Total fatty acids were extracted and quantified using LC-MS method described above. To assess phagocytic activity, the abundance of VLC-PUFAs 32:6, 34:4, 34:5, 34:6, 36:6 was quantified as markers of internalized ROS. All VLC-PUFAs present in ROS were detectable in the cells that were challenged with the cargo, *i.e.* in both ARPE-19 cells and primary bovine RPE cells, an apparent increase was observed for PUFAs longer than 30:4, otherwise not detectable in these cells (**Fig. 2B, C**). We therefore concluded that the lipidomic method is able to detect phagocytosed POS in RPE cells.

Next, we assessed whether the new method is applicable for the detection of the dynamic property of phagocytosis. ARPE-19 cells were challenged with ROS with varying ROS concentrations (0, 10, 20, 40 ROS/cell) and incubation times (0, 0.5, 2, 3.5, 5 hours), and ROS uptake by the cells was quantified by the abundance of marker VLC-PUFAs. The levels of 32:6, 34:4, 34:5, 34:6, 36:6, which were not detected in unchallenged ARPE-19 cells, showed gradual, significant increases of VLC-PUFA content after incubation with increasing amounts of ROS per cell and increasing incubation time (**Fig. 3A**, **B, and Fig. S2A, B, C**). Next, we compared our VLC-PUFA-based assay with the current standard fluorescent phagocytosis assay (Mazzoni, Mao et al. 2019). To do so, ARPE-19 cells were challenged with fluorescently labeled ROS (FITC-ROS) using an optimized concentration of ROS (20 ROS/cell) and incubated for 2 and 5 hours. Following standard protocol (Mao and Finnemann 2012), after fixation and without permeabilization, the cells were briefly stained with an antibody against the C-terminal nine amino acids of bovine rhodopsin (1D4). Internalized FITC-ROS appear as green particles on fluorescence microscopy, whereas surface-bound ROS appear yellow, due to the overlapping FITC- and secondary antibody (red)- derived fluorescence signals, (**Fig. 3C**). Fluorescence-based quantification showed that the number of engulfed ROS increased from 21.01±10.49 to 32.12±8.280 (~53% increase) from 2 to 5 hours when incubated with 20 ROS/cell, (**Fig. 3D, E**). In the same conditions, VLC-PUFAs-based quantification showed increases of up to 6 times in the peak areas of 32:6 - 36:6 from 2 h to 5 h in ARPE-19 cells (**Fig. 3B**).

Validation of the VLC-PUFA-based assay

Lastly, we evaluated whether the VLC-PUFA-based assay could detect impaired RPE phagocytosis secondary to knockdown of genes known to be key molecules in the binding and engulfment of ROS, namely MERTK, GAS6, and MFGE8 (Hall, Prieto et al. 2001, Finnemann and Nandrot 2006, Nandrot, Anand et al. 2007, Law, Parinot et al. 2015). We performed *MERTK/GAS6/MFGE8* triple knockdown in ARPE19 cells and detected 50%, 90%, and 60% knockdown of *MERTK*, *GAS6*, and *MFGE8* mRNA, respectively (**Fig. 4A**). Next, wildtype and triple knockdown (triple KD) ARPE-19 cells were exposed to 10 ROS/cell, and the VLC-PUFA content was measured after 2 hours. The quantification of marker VLC-PUFAs 32:6, 34:4, 34:5, 34:6 and 36:6 decreased 84.82%, 76.63%, 94.70%, 76.50%, 77.40%, respectively, (82.01%±7.90%) in triple KD cells when compared to the control group. The opsin immunoblot-based method indicated a decrease of ~91% of opsin content (1D4) from internalized ROS in triple KD cells. This decrease was consistent with the result obtained by the VLC-PUFA-based assay, indicating the validity of the proposed method.

DISCUSSION

Currently, several common techniques are used to study RPE phagocytosis by measuring POS uptake in cultured RPE cells. However, these techniques possess several disadvantages that limit their interexperimental reliability and high-throughput applicability. In this paper, we present a novel VLC-PUFA-based approach for quantifying RPE phagocytic function that detected ROS uptake by RPE cells at varying ROS concentrations and incubation times, offering a robust, quantifiable, and unbiased assay for high-throughput screening.

VLC-PUFAs are abundant in the outer segment of photoreceptors, where they are especially enriched in the center of the photoreceptor discs, in close proximity to rhodopsin (Sander, Sears et al. 2021). This specific localization most probably provides a highly fluid environment for proteins involved in the visual cycle and residing in these membranes. In the process of daily renewal, ~10% of the outer segment is phagocytosed by RPE, therefore enriching the RPE cells in VLC-PUFAs. As mentioned above, VLC-PUFAs are recycled back to the photoreceptors; however, it is not clear whether RPE cells also synthetize VLC-PUFAs endogenously. To investigate this, we compared the VLC-PUFA profiles of RPE cells isolated directly from the bovine retina, and therefore engaged in the diurnal cycle of phagocytosis, and primary RPE cells, cultured *in vitro* for several days without the presence of outer segments. Our data unequivocally show that, although RPE cells express genes involved in the elongation of long-chain PUFAs (*ELOVL2* and *ELOVL4*), they do not maintain detectable levels of VLC-PUFAs themselves (**Fig. 1D, inset**).

With this very sensitive method of detection and quantification of VLC-PUFAs in hand, we then applied this method as a tool for quantifying phagocytosis activity. Indeed, using isolated bovine ROS and several different incubation conditions, we could detect significant increases in VLC-PUFA content in RPE cells after ROS challenge (**Fig. 3A, B, F, G** and **Fig S2B, C**), which we could confirm with the standard assays (**Fig. 3D, E**). Therefore, our new approach can be used as an orthogonal, yet more sensitive, method of quantification that is complementary to the observations obtained by other assays.

Interestingly, the VLC-PUFA-based method was more sensitive than the fluorescence-based assay when quantifying ROS uptake by ARPE-19 cells incubated with 20 ROS/cell for 2 and 5 hours. Although the two methods both measured an increased phagocytic trend when increasing the ROS incubation time, the fold change is much higher when evaluated by the new VLC-PUFA-based quantification. Considering the high sensitivity and wide linear range of Mass Spectrometry, this VLC-PUFAs-based quantification may represent the optimal method to measure large range of phenotypes and defects in phagocytosis.

Finally, we decided to test whether the VLC-PUFA-based assay is able to detect defects in phagocytosis caused by lack of key regulators of the process. Mer tyrosine kinase (MERTK) is essential for the efficient engulfment of ROS by RPE (Finnemann and Nandrot 2006) and mutations in MERTK have been identified in patients with retinitis pigmentosa (Gal, Li et al. 2000, Al-khersan, Shah et al. 2017, Tagawa, Ikeda et al. 2021) Growth arrest-specific protein 6 (GAS6) specifically and selectively stimulates phagocytosis in cultured rat RPE cells by binding to MERTK on the surface of RPE, leading to the phosphorylation and activation of MERTK (Hall, Prieto et al. 2001, Law, Parinot et al. 2015). Milk

fat globule-EGF 8 (MFG-E8), which localizes to the subretinal space in the retina, can bind to αvβ5 receptors of the RPE and stimulate RPE phagocytosis in the retina(Nandrot, Anand et al. 2007). MFG-E8-deficient cultured primary RPE showed impaired binding and engulfment of isolated POS(Nandrot, Anand et al. 2007). Triple knockdown of *MERTK*, *GAS6*, and *MFG-E8* in ARPE-19 cells impaired phagocytosis by causing defects in the recognition and binding steps. By using the proposed VLC-PUFA-based assay, we showed a remarkable decrease of VLC-PUFAs in triple KD cells when compared to the control group (**Fig. 4B**). Compared to the standard methods (*e.g*. **Fig. 4C, D)**, this new method is directly quantifiable, unbiased, and more sensitive, due to the application of mass spectrometry. Also, since different VLC-PUFAs are used for quantification in one sample, quantification results can be presented for each VLC-PUFA (**Fig. 4B**) or only one FA can be used for a larger number of samples. Therefore, the proposed phagocytosis assay enables high-throughput RPE studies, such as pharmacological or genetic screening, combined with the application of Ultra Performance Liquid Chromatography (UPLC) and high-resolution Mass Spectrometry.

In sum, we present a highly adaptable method for unbiased quantification of RPE phagocytosis through LC-MS and detection of VLC-PUFAs present in POS. The next challenge is to apply this quantitative method for *in vivo* studies.

ACKNOWLEDGMENTS

Authors would like to thank Dr. Huajun Yan for providing primary bovine RPE cells for experiments.

AUTHOR CONTRIBUTIONS

DS-K - Conceptualization, data analysis, writing, editing, providing funding; FG - experiments, data analysis, writing, editing; ET - experiments, data analysis, writing, editing: FG and ET - equally contributed.

FUNDING

Research in the DS-K laboratory is funded by NIH R01EY027011, Thome Foundation and BrightFocus Foundation in part by an unrestricted grant from Research to Prevent Blindness (New York, NY, United States) awarded to Department of Ophthalmology, UC Irvine. ET is funded by the T32GM008620 awarded to University of California Irvine.

DISCLOSURE

DS-K is a scientific advisor of *Visgenx, Inc.*

FIGURE LEGENDS

Figure 1. LC-MS method to detect LC-PUFAs and VLC-PUFAs.

A. Workflow for lipid purification and fatty acid extraction from cells and tissue. **B.** Total ion (TIC) and extracted ion (EIC) mass chromatograms of VLC-PUFAs obtained in FS mode by LC–ESI(-)–MS (FS). IS: internal standard (21:5). **C.** LC-PUFAs and VLC-PUFAs composition in bovine RPE and retina tissues exhibited high abundance of VLC-PUFAs, ranging from 32:4 to 36:6. **D.** LC-PUFAs and VLC-PUFAs composition in cultured RPE cells showed minimal amounts of endogenous VLC-PUFAs, despite expression of fatty acid elongation enzymes ELOVL2 (n=4, SD = 0.1553) and ELOVL4 (n=3, SD = 0.2162) (inset).

Figure 2. VLC-PUFAs-based quantification of phagocytosed ROS in RPE cells

A. RPE cells were challenged with unlabelled ROS. After washing and trypsinization to remove unbound and surface-bound ROS, lipids were purified, fatty acids was extracted and subjected to LC-MS analysis.

LC-PUFA and VLC-PUFA composition of ARPE-19 cells (**B**) and primary bovine RPE cells (**C**) before and after 5 h and 0.5 h incubation, respectively, with ROS. Minimal amounts of endogenous VLC-PUFAs were detected in untreated RPE cells, whereas VLC-PUFAs were highly abundant in RPE cells after ROS incubation.

Figure 3. VLC-PUFAs-based quantification can detect dynamic changes in phagocytosis

Increasing amounts of VLC-PUFAs detected in ARPE-19 cells when challenged with increasing ROS concentrations (**A**) or increasing incubation times (**B**).

C. Fluorescence microscopy can distinguish between surface-bound FITC-ROS, which appear yellow in a color overlay of FITC (green) with secondary antibody (red), and internalized ROS, which appear green.

D. ARPE-19 cells were challenged with FITC-ROS for 2 or 5 hours and incubated with antibody against C-terminal epitope of rhodopsin (1D4). Yellow arrows indicate bound ROS, while white arrowheads indicate internalized ROS, which are only visible in the FITC image. (scale bar = 20μm)

E. Fluorescence imaging quantification of internalized ROS per cell nuclei (*n*=9 in each group).

Increasing amounts of VLC-PUFAs measured in primary bovine RPE cells when challenged with increasing ROS concentrations (**F**) or increasing incubation times (**G**).

Figure 4. VLC-PUFAs-based quantification can detect impaired phagocytosis.

A. MerTK, GAS6, MFGE8 mRNA knockdown efficiency measured by RT-qPCR relative to TBP expression.

B. Significantly lower levels of VLC-PUFAs detected in triple knockdown ARPE-19 cells challenged with 10 ROS/cell for 2 hours. (** = $p<0.01$, *** = $p<0.001$)

C. Opsin immunoblotting analysis of ROS phagocytosis can distinguish between internalized ROS (treated with EDTA before lysis) and total ROS (without EDTA treatment).

Triple KD cells show less internalized (int) and total (tot) ROS after 2 hours (**D**), as quantified by opsin content (**E**). Ponceau S staining was used for total protein normalization. * = non-specific bands

Supplementary Figure 1. Identification and quantification of VLC-PUFAs by LC-MS and LC-MS/MS method.

Peak clusters with a mass difference of 14 Da corresponding to CH_2 in parallel reaction monitoring (PRM) fragment ion chromatograms of 32: 6 (**A**) and 34:4 (**B**) from bovine retina extract.

C. Linearity and linear range for 32:6 in FS mode. Linear correlation coefficient = 0.994 from 50 nmol/L to 1000 nmol/L, and the limit of quantification of 32:6 = 5 nmol/L.

D. The standard deviations of the peak area of the given VLC-PUFAs from bovine retina extract were below 15% (n=5).

E. LC-PUFAs and VLC-PUFAs composition in mouse retina, eyecup and RPE cells exhibited high abundance of VLC-PUFAs, ranging from 32:6 to 36:6.

Supplementary Figure 2. VLC-PUFAs-based quantification can detect dynamic changes in phagocytosis

A. Extracted ion (EIC) mass chromatograms of marker VLC-PUFAs obtained in FS mode by LC–ESI(-)–MS (FS) after incubating with 20 ROS/cell for 2 and 5 hours.

Quantification of phagocytosis was performed by using 34:4 as one of ROS marker VLC-PUFAs when ARPE-19 cells were challenged with increasing ROS concentrations (B) or increasing incubation times (C). (* = $p<0.05$, ** = $p<0.01$)

REFERENCES

Agbaga, M.-P., R. S. Brush, M. N. A. Mandal, K. Henry, M. H. Elliott and R. E. Anderson (2008). "Role of Stargardt-3 macular dystrophy protein (ELOVL4) in the biosynthesis of very long chain fatty acids." Proceedings of the National Academy of Sciences **105**(35): 12843-12848.

Al-khersan, H., K. P. Shah, S. C. Jung, A. Rodriguez, R. K. Madduri and M. A. Grassi (2017). "A novel MERTK mutation causing retinitis pigmentosa." Graefe's Archive for Clinical and Experimental Ophthalmology **255**(8): 1613-1619.

Esteve-Rudd, J., V. S. Lopes, M. Jiang and D. S. Williams (2014). In vivo and in vitro monitoring of phagosome maturation in retinal pigment epithelium cells. Retinal Degenerative Diseases, Springer**:** 85-90.

Finnemann, S. C. and E. F. Nandrot (2006). Mertk Activation During RPE Phagocytosis in Vivo Requires αVβ5 Integrin. Retinal Degenerative Diseases, Boston, MA, Springer US.

Gal, A., Y. Li, D. A. Thompson, J. Weir, U. Orth, S. G. Jacobson, E. Apfelstedt-Sylla and D. Vollrath (2000). "Mutations in MERTK, the human orthologue of the RCS rat retinal dystrophy gene, cause retinitis pigmentosa." Nature genetics **26**(3): 270-271.

Hall, M. O., A. L. Prieto, M. S. Obin, T. A. Abrams, B. L. Burgess, M. J. Heeb and B. J. Agnew (2001). "Outer Segment Phagocytosis by Cultured Retinal Pigment Epithelial Cells Requires Gas6." Experimental Eye Research **73**(4): 509-520.

Hook, G. R. and C. O. Odeyale (1989). "Confocal scanning fluorescence microscopy: a new method for phagocytosis research." Journal of leukocyte biology **45**(4): 277-282.

Inana, G., C. Murat, W. An, X. Yao, I. R. Harris and J. Cao (2018). "RPE phagocytic function declines in age-related macular degeneration and is rescued by human umbilical tissue derived cells." Journal of translational medicine **16**(1): 1-15.

LaVail, M. M. (1976). "Rod outer segment disk shedding in rat retina: relationship to cyclic lighting." Science **194**(4269): 1071-1074.

Law, A.-L., C. Parinot, J. Chatagnon, B. Gravez, J.-A. Sahel, S. S. Bhattacharya and E. F. Nandrot (2015). "Cleavage of Mer Tyrosine Kinase (MerTK) from the Cell Surface Contributes to the Regulation of Retinal Phagocytosis*." Journal of Biological Chemistry **290**(8): 4941-4952.

Lewandowski, D., C. L. Sander, A. Tworak, F. Gao, Q. Xu and D. Skowronska-Krawczyk (2021). "Dynamic lipid turnover in photoreceptors and retinal pigment epithelium throughout life." Progress in Retinal and Eye Research: 101037.

Lewis, T. R., S. R. Kundinger, B. A. Link, C. Insinna and J. C. Besharse (2018). "Kif17 phosphorylation regulates photoreceptor outer segment turnover." BMC cell biology **19**(1): 1-16.

Mao, Y. and S. C. Finnemann (2012). Analysis of photoreceptor outer segment phagocytosis by RPE cells in culture. Retinal Degeneration, Springer**:** 285-295.

Mazzoni, F., Y. Mao and S. C. Finnemann (2019). Advanced Analysis of Photoreceptor Outer Segment Phagocytosis by RPE Cells in Culture. Retinal Degeneration: Methods and Protocols. B. H. F. Weber and T. Langmann. New York, NY, Springer New York**:** 95-108.

Nandrot, E. F., M. Anand, D. Almeida, K. Atabai, D. Sheppard and S. C. Finnemann (2007). "Essential role for MFG-E8 as ligand for αvβ5 integrin in diurnal retinal phagocytosis." Proceedings of the National Academy of Sciences **104**(29): 12005-12010.

Nandrot, E. F., M. Anand, D. Almeida, K. Atabai, D. Sheppard and S. C. Finnemann (2007). "Essential role for MFG-E8 as ligand for αvβ5 integrin in diurnal retinal phagocytosis." Proceedings of the National Academy of Sciences **104**(29): 12005-12010.

Ramarao, N. and T. F. Meyer (2001). "Helicobacter pylori resists phagocytosis by macrophages: quantitative assessment by confocal microscopy and fluorescence-activated cell sorting." Infection and immunity **69**(4): 2604-2611.

Sander, C. L., A. E. Sears, A. F. Pinto, E. H. Choi, S. Kahremany, F. Gao, D. Salom, H. Jin, E. Pardon and S. Suh (2021). "Nano-scale resolution of native retinal rod disk membranes reveals differences in lipid composition." Journal of Cell Biology **220**(8): e202101063.

Schreiter, S., K. Vafia, R. Barsacchi, S. H. Tsang, M. Bickle, M. Ader, M. O. Karl, E. M. Tanaka and S. Almedawar (2020). "A Human Retinal Pigment Epithelium-Based Screening Platform Reveals Inducers of Photoreceptor Outer Segments Phagocytosis." Stem cell reports **15**(6): 1347-1361.

Sethna, S., T. Chamakkala, X. Gu, T. C. Thompson, G. Cao, M. H. Elliott and S. C. Finnemann (2016). "Regulation of

phagolysosomal digestion by caveolin-1 of the retinal pigment epithelium is essential for vision." Journal of Biological Chemistry **291**(12): 6494-6506.

Sun, K., H. Cai, T. H. Tezel, D. Paik, E. R. Gaillard and L. V. Del Priore (2007). "Bruch's membrane aging decreases phagocytosis of outer segments by retinal pigment epithelium."

Tagawa, M., H. O. Ikeda, Y. Inoue, S. Iwai, Y. Iida, M. Hata, I. Asaka and A. Tsujikawa (2021). "Deterioration of phagocytosis in induced pluripotent stem cell-derived retinal pigment epithelial cells established from patients with retinitis pigmentosa carrying Mer tyrosine kinase mutations." Experimental Eye Research **205**: 108503.

Takashima, S., K. Toyoshi, T. Yamamoto and N. Shimozawa (2020). "Positional determination of the carbon–carbon double bonds in unsaturated fatty acids mediated by solvent plasmatization using LC–MS." Scientific reports **10**(1): 1-14.

Vargas, J. A. and S. C. Finnemann (2022). "Probing Photoreceptor Outer Segment Phagocytosis by the RPE In Vivo: Models and Methodologies." International Journal of Molecular Sciences **23**(7): 3661.

Westenskow, P. D., S. K. Moreno, T. U. Krohne, T. Kurihara, S. Zhu, Z.-n. Zhang, T. Zhao, Y. Xu, S. Ding and M. Friedlander (2012). "Using flow cytometry to compare the dynamics of photoreceptor outer segment phagocytosis in iPS-derived RPE cells." Investigative ophthalmology & visual science **53**(10): 6282-6290.

Young, R. W. (1978). "The daily rhythm of shedding and degradation of rod and cone outer segment membranes in the chick retina." Investigative ophthalmology & visual science **17**(2): 105-116.

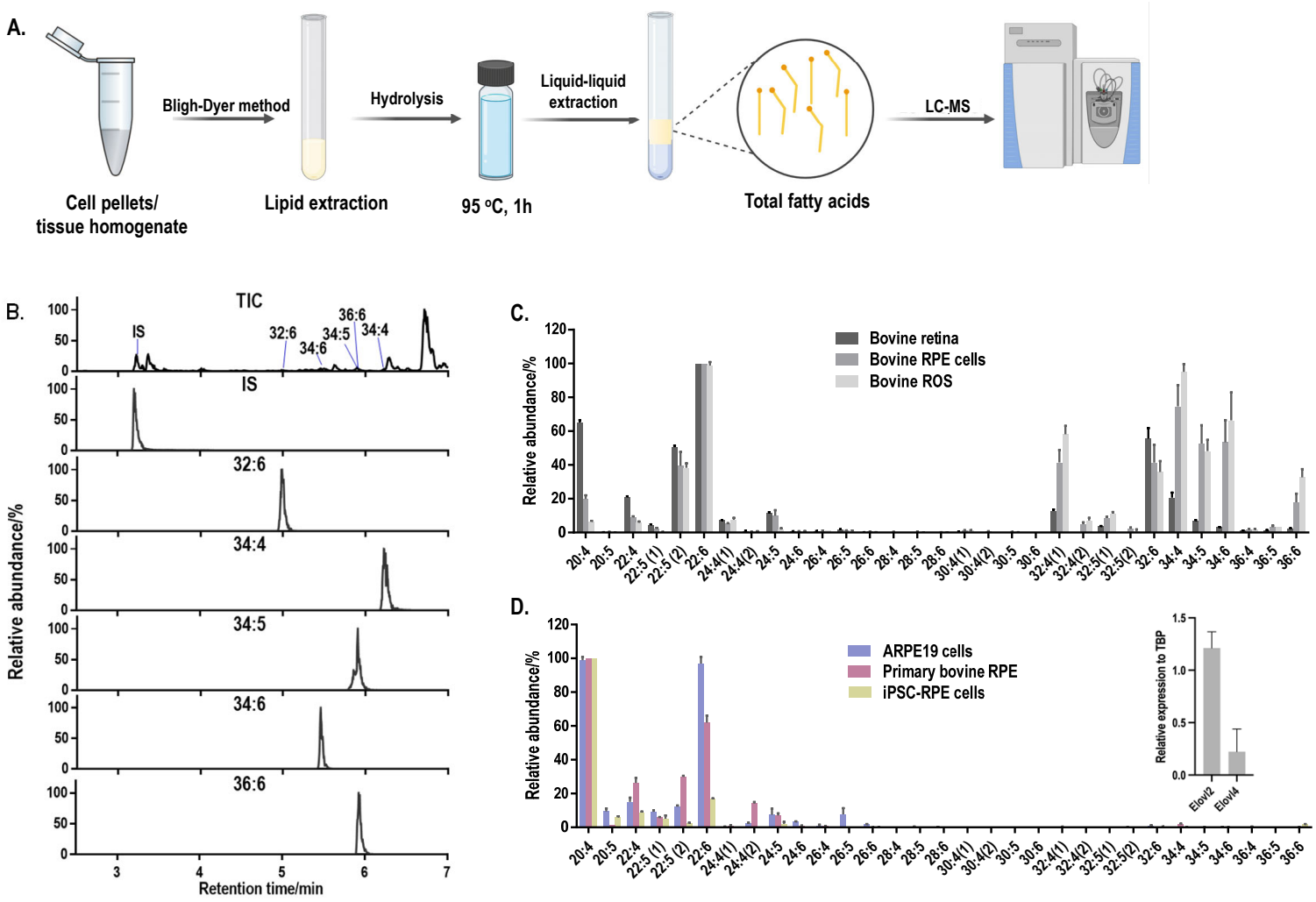

Figure 1. LC-MS method to detect LC-PUFAs and VLC-PUFAs.

A. Workflow for lipid purification and fatty acid extraction from cells and tissue

B. Total ion (TIC) and extracted ion (EIC) mass chromatograms of VLC-PUFAs obtained in FS mode by LC–ESI(-)–MS (FS). IS: internal standard (21:5)

C. LC-PUFAs and VLC-PUFAs composition in bovine RPE and retina tissues exhibited high abundance of VLC-PUFAs, ranging from 32:4 to 36:6.

D. LC-PUFAs and VLC-PUFAs composition in cultured RPE cells showed minimal amounts of endogenous VLC-PUFAs, despite expression of fatty acid elongation enzymes ELOVL2 (n=4, SD = 0.1553) and ELOVL4 (n=3, SD = 0.2162) (**inset**).

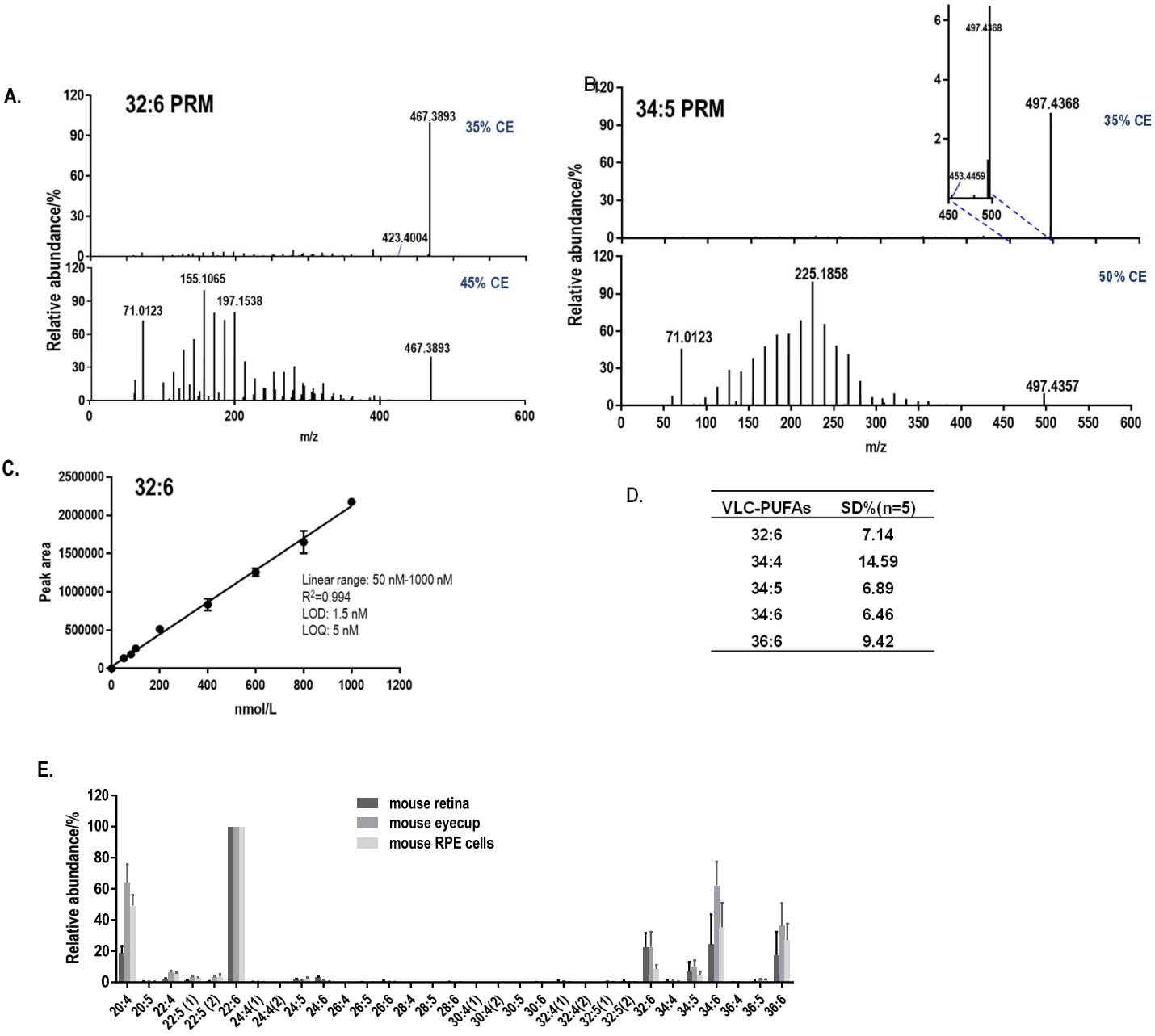

VLC-PUFAs	SD%(n=5)
32:6	7.14
34:4	14.59
34:5	6.89
34:6	6.46
36:6	9.42

Supplementary Figure 1. Identification and quantification of VLC-PUFAs by LC-MS and LC-MS/MS method.

Peak clusters with a mass difference of 14 Da corresponding to CH_2 in parallel reaction monitoring (PRM) fragment ion chromatograms of 32: 6 **(A)** and 34:4 **(B)** from bovine retina extract.

C. Linearity and linear range for 32:6 in FS mode. Linear correlation coefficient = 0.994 from 50 nmol/L to 1000 nmol/L, and the limit of quantification of 32:6 = 5 nmol/L.

D. The standard deviations of the peak area of the given VLC-PUFAs from bovine retina extract were below 15% (n=5).

E. LC-PUFAs and VLC-PUFAs composition in mouse retina, eyecup and RPE cells exhibited high abundance of VLC-PUFAs, ranging from 32:6 to 36:6.

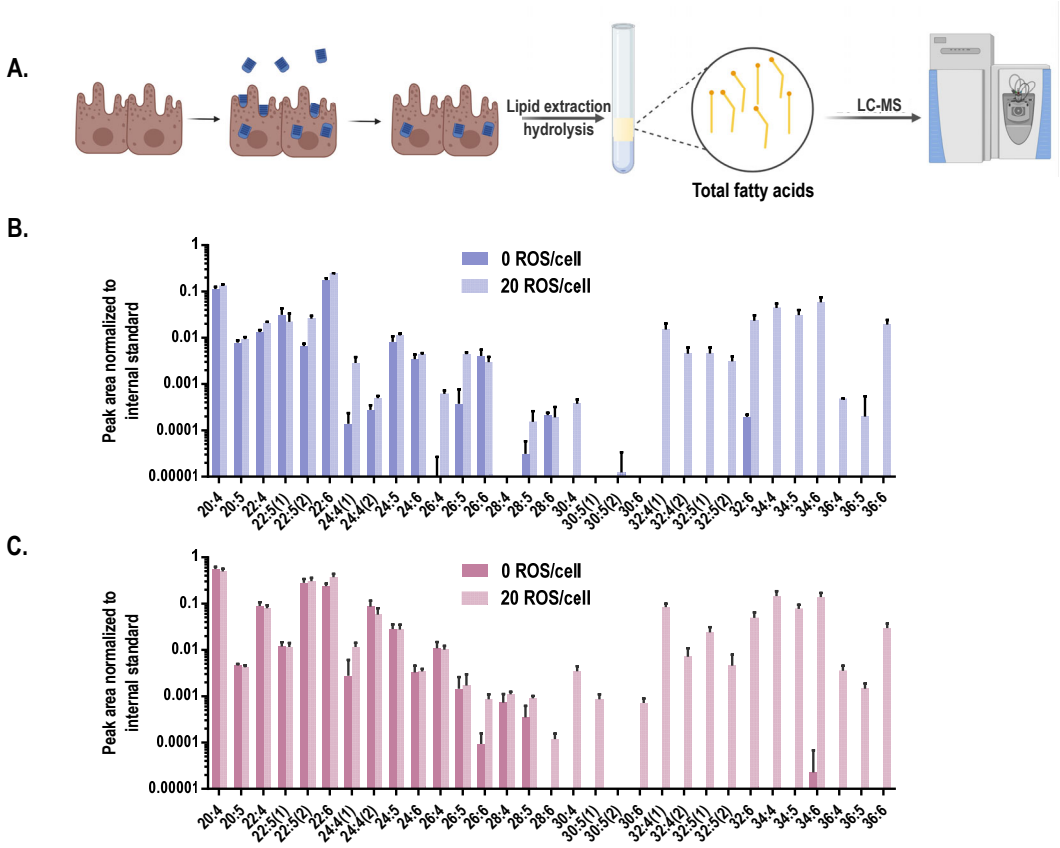

Figure 2. VLC-PUFAs-based quantification of phagocytosed ROS in RPE cells

A. RPE cells were challenged with unlabelled ROS. After washing and trypsinization to remove unbound and surface-bound ROS, lipids were purified, fatty acids was extracted and subjected to LC-MS analysis.
LC-PUFA and VLC-PUFA composition of ARPE-19 cells **(B)** and primary bovine RPE cells **(C)** before and after 5 h and 0.5 h incubation, respectively, with ROS. Minimal amounts of endogenous VLC-PUFAs were detected in untreated RPE cells, whereas VLC-PUFAs were highly abundant in RPE cells after ROS incubation.

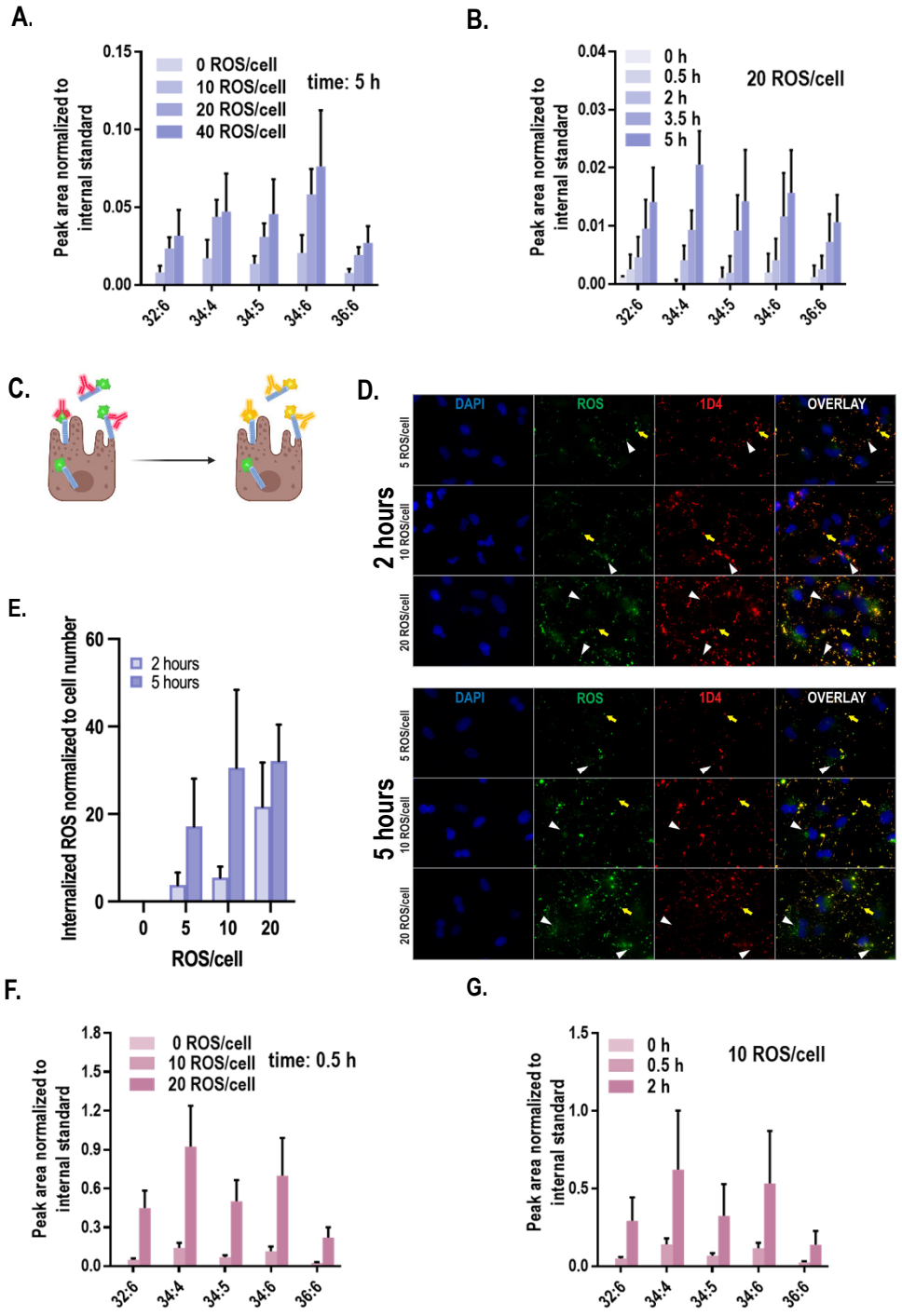

Figure 3. VLC-PUFAs-based quantification can detect dynamic changes in phagocytosis

Increasing amounts of VLC-PUFAs detected in ARPE-19 cells when challenged with increasing ROS concentrations **(A)** or increasing incubation times **(B)**.

C. Fluorescence microscopy can distinguish between surface-bound FITC-ROS, which appear yellow in a color overlay of FITC (green) with secondary antibody (red), and internalized ROS, which appear green.

D. ARPE-19 cells were challenged with FITC-ROS for 2 or 5 hours and incubated with antibody against C-terminal epitope of rhodopsin (1D4). Yellow arrows indicate bound ROS, while white arrowheads indicate internalized ROS, which are only visible in the FITC image. (scale bar = 20μm)

E. Fluorescence imaging quantification of internalized ROS per cell nuclei (*n*=9 in each group).

Increasing amounts of VLC-PUFAs measured in primary bovine RPE cells when challenged with increasing ROS concentrations **(F)** or increasing incubation times **(G)**.

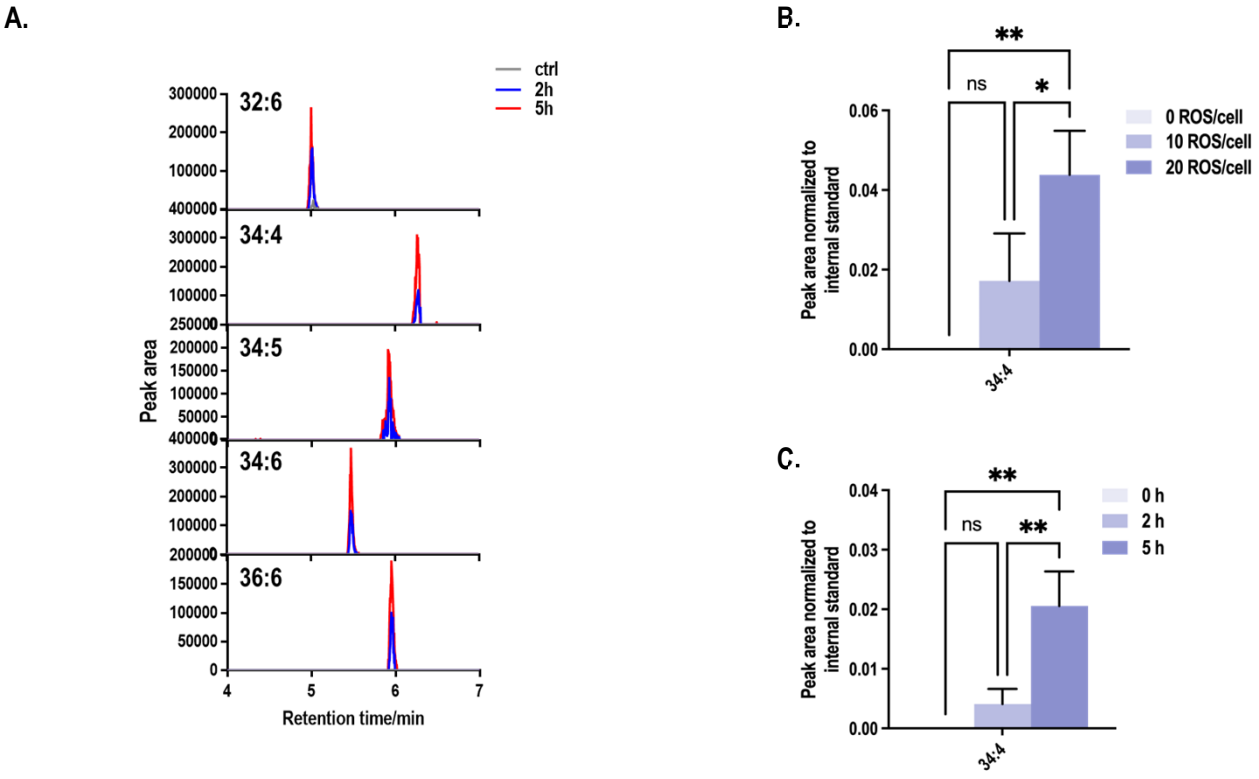

Supplementary Figure 2. VLC-PUFAs-based quantification can detect dynamic changes in phagocytosis

A. Extracted ion (EIC) mass chromatograms of marker VLC-PUFAs obtained in FS mode by LC–ESI(-)–MS (FS) after incubating with 20 ROS/cell for 2 and 5 hours.

Quantification of phagocytosis was performed by using 34:4 as one of ROS marker VLC-PUFAs when ARPE-19 cells were challenged with increasing ROS concentrations **(B)** or increasing incubation times **(C)**. (* = $p<0.05$, ** = $p<0.01$)

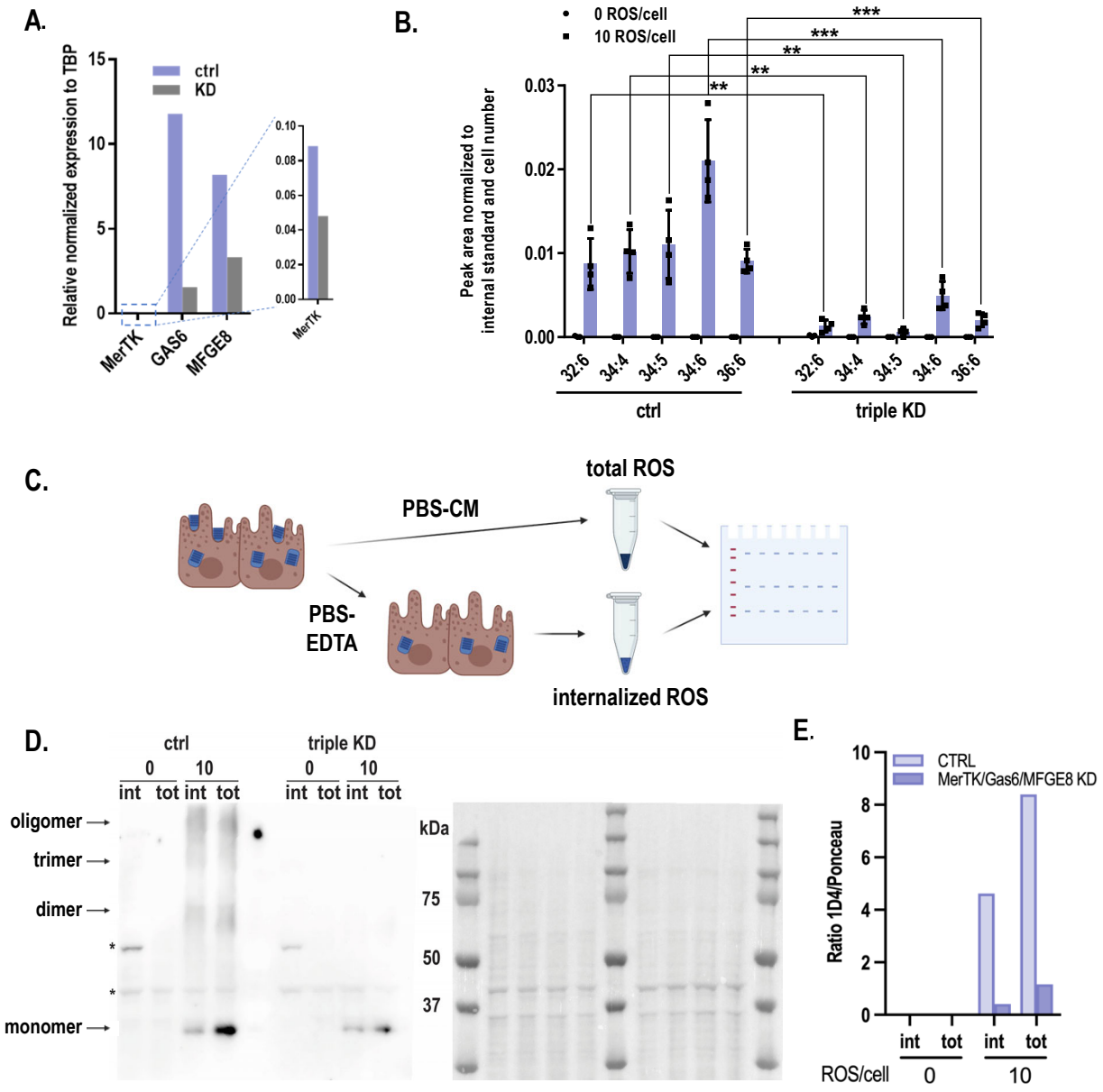

Figure 4. VLC-PUFAs-based quantification can detect impaired phagocytosis.

A. *MerTK*, *GAS6*, *MFGE*8 mRNA knockdown efficiency measured by RT-qPCR relative to TBP expression.

B. Significantly lower levels of VLC-PUFAs detected in triple knockdown ARPE-19 cells challenged with 10 ROS/cell for 2 hours. (** = p<0.01, *** = p<0.001)

C. Opsin immunoblotting analysis of ROS phagocytosis can distinguish between internalized ROS (treated with EDTA before lysis) and total ROS (without EDTA treatment).

Triple KD cells show less internalized (int) and total (tot) ROS after 2 hours **(D)**, as quantified by opsin content **(E)**. Ponceau S staining was used for total protein normalization. * = non-specific bands

Table 1. siRNA and qPCR primer sequences

Gene	siRNA	
MERTK	GAAUCCAAUUGUACCUGA, AAAAACAUCAGGUACAAU	
GAS6	CGAGGACUGUAUCAUCUG, UCAGGUUCAGAUGAUACA	
MFG-E8	GCGGUGCAUGUCAACCU, UCUCAAACAGGUUGACAU	
	qPCR	
Gene	Forward (5'-3')	Reverse (5'-3')
TBP	TGTATCCACAGTGAATCTTGGTT	GGTTCGTGGCTCTCTTATCCTC
MERTK	CAGCAGGATGGAGAACTGGT	TGGACTTGAACAGAGATCCGA
GAS6	CAGCTGCGCTACAACGGT	CCCTGTTGACCTTGATGACC
MFG-E8	CTTTGAGCTACTGGGCTGTGA	GTCTTGTAGCTGCTGGAGGC

Table 2. LC-PUFA and VLC-PUFA composition from bovine retina

FAs	Chemical formula	m/z	Retention time/min
21:5(IS)	C21H32O2	315.233	3.19
20:4	C20H32O2	303.233	3.3
20:5	C20H30O2	301.2173	3.11
22:4	C22H36O2	331.2643	3.58
22:5 (1)	C22H34O2	329.2486	3.35
22:5 (2)	C22H34O2	329.2486	3.44
22:6	C22H32O2	327.233	3.23
24:4(1)	C24H40O2	359.2956	3.91
24:4(2)			4.02
24:5	C24H38O2	357.2799	3.69
24:6	C24H36O2	355.2643	3.45
26:4	C26H44O2	387.3269	4.32
26:5	C26H42O2	385.3112	4.03
26:6	C26H40O2	383.2956	3.73
28:4	C28H48O2	415.3582	4.76
28:5	C28H46O2	413.3425	4.42
28:6	C28H44O2	411.3269	4.12
30:4	C30H52O2	443.3895	5.26
30:5 (1)	C30H50O2	441.3738	4.89
30:5 (2)	C30H50O2	441.3738	4.99
30:6	C30H48O2	439.3582	nd
32:4 (1)	C32H56O2	471.4208	5.76
32:4 (2)	C32H56O2	471.4208	5.91
32:5 (1)	C32H54O2	469.4051	5.34
32:5 (2)	C32H54O2	469.4051	5.45
32:6	C32H52O2	467.3895	5.01
34:4	C34H60O2	499.4521	6.28
34:5	C34H58O2	497.4364	5.89
34:6	C34H56O2	495.4208	5.46
36:4	C36H64O2	527.4834	6.67
36:5	C36H62O2	525.4677	6.34
36:6	C36H60O2	523.4521	5.94

nd = non-detected